

On-Chip Antenna Designs for UHF RFID

Jingtian XI, Na YAN, Hao MIN

Auto-ID Labs White Paper WP-HARDWARE-044



Jingtian XI
Ph.D. candidate
Auto-ID Labs at Fudan Univ.



Na YAN
Ph.D.
Auto-ID Labs at Fudan Univ.



Hao MIN
Professor
Research Director
Auto-ID Labs at Fudan Univ.

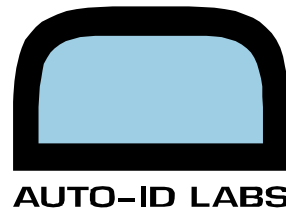
Contact:

Auto-ID Labs at Fudan Univ.
No. 825, Zhangheng Road, Zhangjiang High-Tech Park,
Shanghai, China, 201203

Phone: +86 21 5135 5328
E-Mail: jtxi@fudan.edu.cn
Internet: www.autoidlabs.org

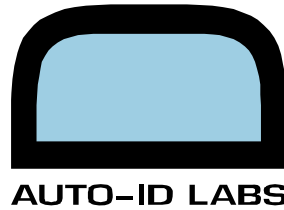
Copyright © 2007 IEEE. Reprinted from the PerCom 2007 workshops proceedings.

This material is posted here with permission of the IEEE. Such permission of the IEEE does not in any way imply IEEE endorsement of any of Auto-ID Lab's products or services. Internal or personal use of this material is permitted. However, permission to reprint/republish this material for advertising or promotional purposes or for creating new collective works for resale or redistribution must be obtained from the IEEE by writing to pubs-permissions@ieee.org.



Index

| | |
|---|----|
| Abstract | 3 |
| 1. Introduction..... | 3 |
| 2. Electromagnetic Propagation and Coupling | 4 |
| 2.1. Maxwell's equations | |
| 2.2. Field regions of antennas | |
| 3. Modeling of On-Chip Antennas | 6 |
| 3.1. Choice of antenna type | |
| 3.2. OCA models | |
| 4. Design and Simulation of OCA..... | 8 |
| 5. Measurement and Test..... | 9 |
| 6. Conclusions | 11 |
| References | 12 |



Abstract

Item-level tagging (ILT) has put a strict demand on the size and cost of tags. Near-field UHF RFID is believed to be one solution to implement ILT. To reduce the size and cost of tags to the minimum, on-chip antennas (OCA) utilizing near-field coupling are studied in this paper. Full-wave electromagnetic solvers are used to aid OCA design, and measurement results are presented to demonstrate the feasibility of UHF tags with OCA embedded.

1. Introduction

The surge of interests in item-level tagging has been among the top 10 RFID trends in 2006, because industries like apparel, consumer electronics, and pharmaceuticals become eager to track and trace their goods, which are often targets of theft or counterfeit. Item means the smallest unit of goods. Further understanding of ILT can be achieved with the comparison of different tagging levels [1]. It is reasonable to say that the biggest payback in implementing RFID is in ILT.

The criteria for successful ILT are born in industries. Below are the demands from Wal-Mart.

- Low cost;
- Strictly limited tag size;
- Short read range or hybrid ranges (short for items, long for cases and pallets);
- Fast reading ability;
- Follow a globally accepted protocol.

EPCglobal has organized a special work group to compare different solutions for ILT. Now UHF takes the lead. More accurately speaking, it is to use UHF in the near-field. There are four approaches to implement near-field UHF RFID systems using existing readers and tag chips [2]. Near-field tag antennas are needed to turn out the best performance.

The term on-chip antennas is used for a class of radiating structures where devices such as solid-state oscillators, detectors, phase shifters and filters are integrated with the radiating elements on the same substrate, typically in monolithic form [3]. OCA has the obvious advantages of compactness, reliability, reproducibility and, if fabricated in large numbers, of low cost.

OCA can be utilized in a large variety of applications such as true single-chip radio for general purpose communications, RFID tags, intra-chip and inter-chip data communications, RF sensors/radars, clock distribution, car anti-collision systems, wireless LAN devices,

wireless personal area network (WPAN) applications, etc. RFID tags with OCA embedded have been reported at HF and MW bands [4-6].

This paper is to develop OCA for UHF RFID tags, which utilizes the near-field of antennas and is suitable for ILT. We begin with an overview of electromagnetic theories for a better understanding of OCA in section 2. OCA modeling is discussed in section 3. Section 4 further deals with the design of OCA with simulation aided. The fabrication and measurement of OCA are presented in section 5. Finally, several corresponding conclusions are drawn in section 6.

2. Electromagnetic Propagation and Coupling

2.1. Maxwell's equations

The complete laws of electrodynamics were first assembled in 1873 by Maxwell in a precise and accurate form, namely, Maxwell's equations. This whitepaper is devoted to the exposition and explanation of Maxwell's equations in the following mathematical forms.

$$\nabla \times \vec{H} = \frac{\partial \vec{D}}{\partial t} + \vec{J} \quad (1a)$$

$$\nabla \times \vec{E} = -\frac{\partial \vec{B}}{\partial t} \quad (1b)$$

$$\nabla \cdot \vec{D} = \rho \quad (1c)$$

$$\nabla \cdot \vec{B} = 0 \quad (1d)$$

Eq.(1a) is Ampere's law or the generalized Ampere circuit law. Eq.(1b) is Faraday's law or Faraday's magnetic induction law. Eq.(1c) is Gauss' law for electric fields. Eq. (1d) is Gauss' law for magnetic fields [7].

Faraday's law states that surrounding a time-varying magnetic field, time-varying electric fields are produced. With the displacement current term in Ampere's law, Ampere's law states that around time-varying electric fields, time-varying magnetic fields are produced. This interrelationship between time-varying electric fields and magnetic fields constitutes the foundation of electromagnetic propagation.

2.2. Field regions of antennas

The space surrounding an antenna is usually divided into three regions: reactive near-field, radiating near-field and far field, as illustrated in Fig.1.

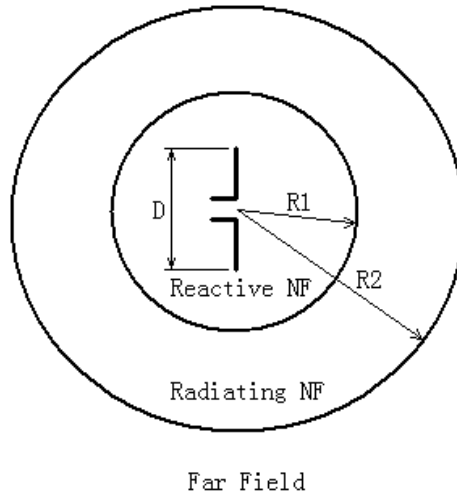


Fig.1: Field regions of antennas

Reactive near-field is the region immediately surrounding the antenna wherein the reactive field predominates. The Poynting vector is predominately imaginary. Reactive near-field has all three components in spherical coordinates (theta, phi, r), and decays more rapidly than $1/r$.

Radiating near-field is the region of the field of an antenna between the reactive near-field region and the far field region wherein radiation field predominates (while there still coexists reactive field). In the radiating near-field, the radial field component may be appreciable, and the field pattern is dependent upon the distance from the antenna.

Far-field is the region of the field of an antenna where the field pattern is essentially independent of the distance from the antenna. And the Poynting vector is real. Far-field decays as $1/r$ and has only two components in spherical coordinates (theta, phi). In other words, the field components are essentially transverse.

Although no abrupt changes in the field configurations are noted as the boundaries are crossed, there are distinct differences among them. The boundaries separating these regions are not unique, although various criteria have been established [8].

One common accepted definition of boundaries is $R_1 = 0.62\sqrt{D^3/\lambda}$, $R_2 = 2D^2/\lambda$, where D is the largest dimension of the antenna. To be valid, D must be large compared to the wavelength ($D > \lambda$). For electrically small antennas, the boundary separates the (reactive) near-field and the far-field is taken to exist at a distance $\lambda/2\pi$ from the antenna surface, and the radiating near-field of electrically small antennas may not exist due to the merge of the other two field regions.

Near-field UHF takes advantage of fields in the near-field region instead of waves in the far-field region. The quasi-static characteristic of the near-field is the result of the antenna geometry in combination with the carrier frequency of the transmitter [9].

3. Modeling of On-Chip Antennas

3.1. Choice of antenna types

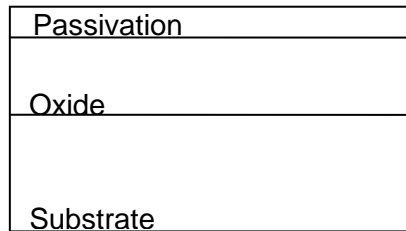


Fig.2: Sketch of dielectric layers

Tab.1: Wavelength as a function of frequency and material

| Frequency | Air | Oxide | Si-sub |
|----------------|---------|---------|--------|
| HF (13.56 MHz) | 22.1 m | 11.1 m | 6.4 m |
| UHF (900 MHz) | 33.3 cm | 16.7 cm | 9.6 cm |
| MW (2.45 GHz) | 12.2 cm | 6.1 cm | 3.5 cm |

A simplified stack of dielectric layers of commercial CMOS process is illustrated in Fig.2. OCA can be thought as immersed in the oxide layer. Therefore, the guided wavelength of oxide has the largest influence on OCA. OCA at UHF is electrically small, since die sizes are in the order of mm, which are far less than the guided wavelength of oxide as listed in Tab.1 (where the permittivities of oxide and silicon substrate are respectively 4 and 12, relative to air).

It is generally accepted that electrically small antennas store (on time average) much more energy than they radiate. This large ratio of time-average, non-propagating stored energy to radiated power usually makes electrically small antennas poor radiators in the far-field. Fortunately, we could take advantage of the quasi-static characteristic of the near-field of electrically small antennas, like what near-field magnetic communication does [10]. As a result, electrically small loop antennas seem to be a good and may be the unique choice for OCA at UHF band.

3.2. OCA models

In order to integrate OCA with tag circuits, we need to describe OCA in its equivalent circuit. Fig.3 shows the Thevenin equivalent for small loops in receiving mode, where R_r is the radiation resistance, R_L is the loss resistance of loop conductor, L_A is the external inductance of loop antenna, and V_{oc} is the open-circuit voltage induced [11].

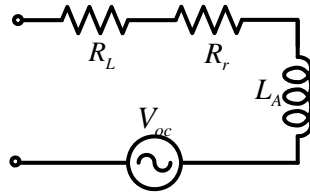


Fig.3: Thevenin equivalent for small loops in receiving mode

There are two problems with the equivalent circuit above when applying it to OCA modeling. First, the closed-form expressions of inductances cannot be easily extended to fit multi-turn loops. Second, the loss is quite underestimated due to lossy substrate. While the first problem will be solved using Greenhouse's method, the latter is really a headache. Recently we use the models of integrated spiral inductors to solve this problem, for example, the single-pi model as illustrated in Fig.4 and Tab.2 [12]. This is reasonable since OCA of small loop kind is primary inductive and resembles the shape of integrated spiral inductors.

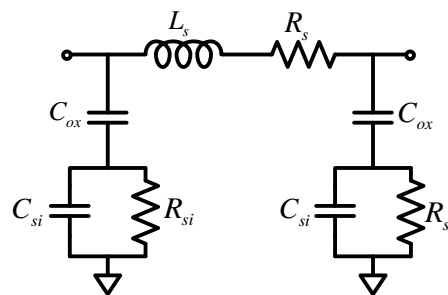


Fig.4: Single-pi model of integrated spiral inductors

Tab.2: Elements of single-pi model

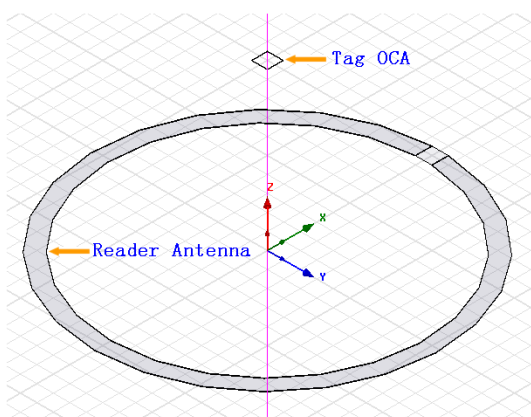
| Name | Definition | Originality |
|-----------------|--|--|
| L _s | Series inductance | Ampere's law |
| R _s | Series resistance | Current distribution in the metal trace |
| C _s | Series capacitance | Overlap between the spiral and the underpass mainly, and the crosstalk between adjacent turns |
| C _{ox} | The oxide capacitance between the spiral and the silicon substrate | Plate capacitor formed by the spiral and the lossy substrate |
| R _{si} | Resistance of the silicon substrate | The silicon conductivity which is predominately determined by the majority carrier concentration |
| C _{si} | Capacitance of the silicon substrate | High-frequency capacitive effects occurring in the semiconductor |

4. Design and Simulation of On-Chip Antennas

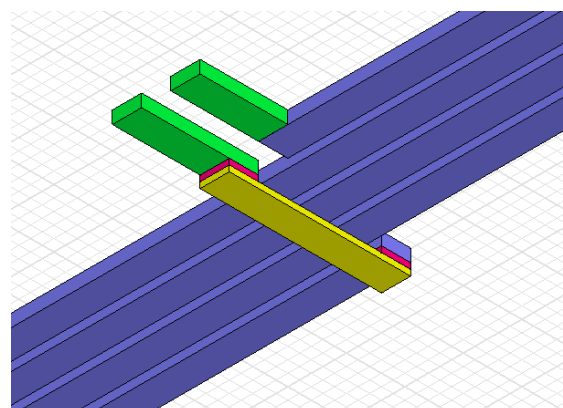
Before starting to develop OCA, we need to obtain its spec. The common situation is that we only have the input impedance of tag circuits and the required system performance. The way to derive the spec of OCA for UHF RFID is similar to that of magnetic-coupling HF RFID systems, which has been investigated adequately [13-15] and is summarized below.

- The tag antenna should be designed in combination with reader antenna.
- The tag antenna should be at resonance to enlarge the input voltage to tag circuits at the desired frequency.
- The quality factor of the tag antenna should not be too large in order to meet a sufficient bandwidth.
- The impedance of the tag antenna needs to be matched with tag circuits so as to maximize the delivering power.

However, we need to pay special attention to OCA designs, since they appear different features compared to common HF tag antennas. First, the OCA inductance needed to resonate with tag circuits usually is too large to be achieved on chip, so tuning capacitances may be added. Second, the quality factor of OCA is much smaller than what we meet in HF RFID systems because of more serious losses of metals and low-resistivity substrates; it alleviates the problem of bandwidth but demands a larger induced voltage in order to guarantee enough input voltage to tag circuits. Third, since the matching network between OCA and tag circuits should be constructed exclusively by capacitors, a perfect match is hard to achieve.



(a) Overview of the simulation geometry



(b) Details about the port of tag OCA

Fig.5: Simulation of near-field coupling with HFSS

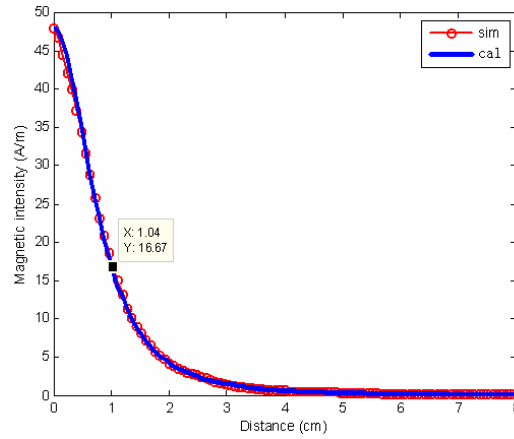


Fig.6: Simulation results of magnetic fields produced by the reader antenna

Although there are several formulas to predict the near-field magnetic fields produced by some simple antennas, they are generally estimations, let alone the near-field of other complicated antennas. Full wave electromagnetic field solvers are employed to handle this embarrassment and fill the blank. As illustrated in Fig.5, the near-field coupling between reader antenna and OCA is studied with HFSS. Fig.6 shows a good match between simulation and calculation for magnetic fields produced by a small loop reader antenna. The calculation is based on the following equation,

$$H = \frac{INR^2}{2\sqrt{(R^2 + d^2)^3}} \quad (2)$$

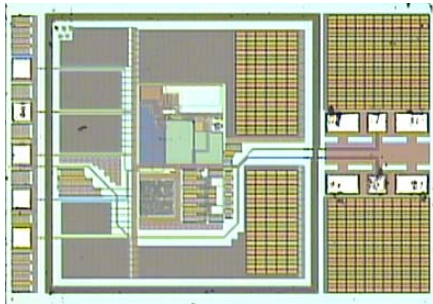
where I is the current the small loop carries, N is the number of turns, R is the radius of the circular loop, and d is the distance away from the centre of the loop along its axis. And the setup is I=0.95A (max), N=1, R=1cm. According to Fig.6, a magnetic field of peak value 17A/m is achieved at a distance 1cm from the reader antenna, where the induced voltage on tag OCA is about 0.5V.

5. Measurement and Test

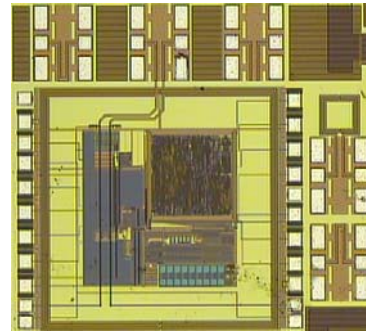
Two OCA prototypes have been fabricated using 0.18um CMOS process. They are both in a square shape encircling tag circuits as illustrated in Fig.7. Their detailed layout parameters are listed in Tab.3, where W is line width, S is space between adjacent metal lines, N is number of turns, Dout is the outmost diameter.

Tab.3: Layout parameters of OCA prototypes

| No. | W (um) | S (um) | N | Dout (mm) |
|-------|--------|--------|---|-----------|
| OCA 1 | 5 | 1.5 | 4 | 1 |
| OCA 2 | 10 | 1.5 | 4 | 1.2 |

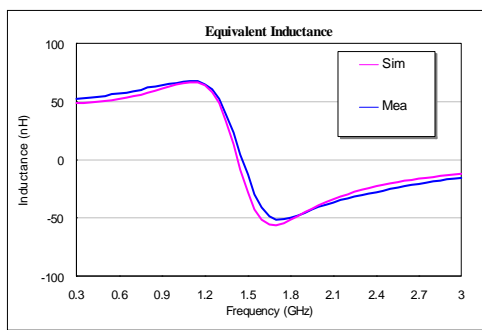


(a) OCA 1

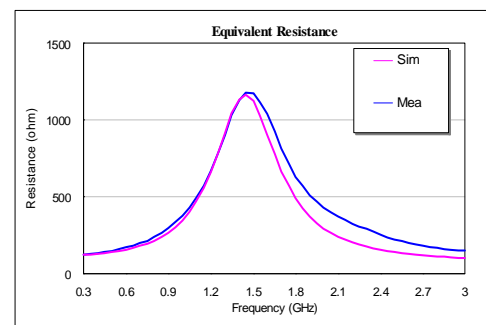


(b) OCA 2

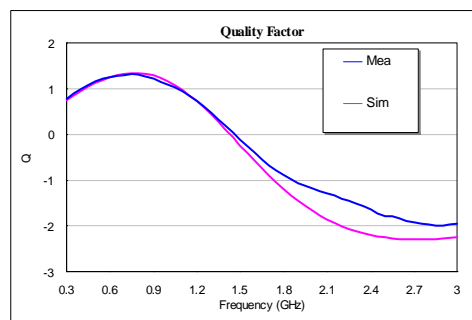
Fig.7: Microphotographs of OCA prototypes



(a) Equivalent inductance



(b) Equivalent resistance



(c) Equivalent quality factor

Fig.8: Comparison between simulation and measurement of OCA 1

The simulation of OCA 1 is compared to its measurement, as illustrated in Fig.8 and summarized in Tab.4. A good match is achieved between simulation and measurement below the self resonant frequency. Since the input impedance of OCA 1 is quite different from that of common tags, a matching network constructed exclusively by capacitor(s) is required. Although the equivalent quality factor is small, OCA 1 is able to provide an input voltage near 0.7V, which is promising for tag circuits' working. The input voltage to tag circuits can be further enlarged if we optimize the OCA design, like using thick top metal. Since there is no digital baseband implemented in OCA 1, we cannot obtain the communication range.

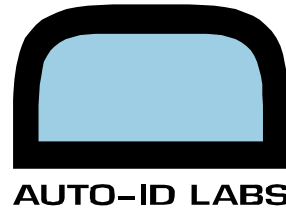
However, we did the experiment by OCA 2, and it turns out that tags with OCA 2 can respond up to 1cm.

Tab.4: Summary of simulation and measurement of OCA 1

| | Leq (nH) | Req (ohm) | Qeq | Self resonant frequency (GHz) |
|-------------|----------|-----------|-------|-------------------------------|
| Simulation | 61.02 | 266.979 | 1.292 | 1.450 |
| Measurement | 64.46 | 297.968 | 1.223 | 1.450 |

6. Conclusions

This paper discusses OCA designs for UHF RFID with the help of full-wave electromagnetic solvers. Measurement results of two fabricated OCA prototypes demonstrate that OCA is able to provide enough input voltage to tag circuits. Future work will include better modelling OCA implemented on lossy substrates and optimization of OCA performance. The work presented in this paper will be a meaningful try to reduce the size and cost of tags to the minimum for ILT.



References

- [1] EPCglobal, "Item-Level Tagging (ILT) Protocol Requirements Document (Version 1.0.0)," Jan. 2006.
- [2] P. V. Nikitin, K. V. S. Rao, and S. Lazar, "An Overview of Near Field UHF RFID," IEEE International Conference on RFID, pp. 167-174, 2007.
- [3] F. K. Schwering, "Millimeter wave antennas," Proceedings of the IEEE, vol. 80, pp. 92-102, 1992.
- [4] A. Abrial, J. Bouvier, M. Renaudin, P. Senn, and P. Vivet, "A new contactless smart card IC using an on-chip antenna and an asynchronous microcontroller," Solid-State Circuits, IEEE Journal of, vol. 36, pp. 1101-1107, 2001.
- [5] M. Usami, "An ultra small RFID chip: mu-chip," RFIC Symposium, IEEE, pp. 241-244, 2004.
- [6] L. H. Guo, A. P. Popov, H. Y. Li, Y. H. Wang, V. Bliznetsov, G. Q. Lo, N. Balasubramanian, and D. L. Kwong, "A small OCA on a $1 \times 0.5\text{-mm}^2$ 2.45-GHz RFID Tag-design and integration based on a CMOS-compatible manufacturing technology," Electron Device Letters, IEEE, vol. 27, pp. 96-98, 2006.
- [7] J. A. Kong, Maxwell Equations, Beijing: Higher Education Press, 2004.
- [8] C. Capps, "Near field or far field?," in *EDN*, Aug. 2001, pp. 95-102.
- [9] P. H. Cole, B. Jamali, D. C. Ranasinghe, "Coupling Relations in RFID Systems," Auto-ID Centre White Paper, 2003.
- [10] R. Bansal, "Near-field magnetic communication," Antennas and Propagation Magazine, IEEE, vol. 46, pp. 114-115, 2004.
- [11] C. A. Balanis, Antenna Theory: Analysis and Design, Second Edition, John Wiley & Sons, 1997.
- [12] C. P. Yue and S. S. Wong, "Physical Modeling of Spiral Inductors on Silicon," IEEE Transactions on Electron Devices, vol. 47, pp. 560-568, 2000.
- [13] Y. Lee, "Antenna Circuit Design for RFID Applications," Microchip Technology Inc. 2003.
- [14] PLC, "13.56 MHz RFID Systems and Antennas Design Guide," Oct. 2004.
- [15] Klaus Finkenzeller, RFID Handbook: Fundamentals and Applications in Contactless Smart Cards and Identification, Second Edition, John Wiley & Sons, 2003.